Molecular Biology of the Cell
Vol. 16, 2207–2217, May 2005

Local Phosphatidylinositol 3,4,5-Trisphosphate Accumulation Recruits Vav2 and Vav3 to Activate Rac1/Cdc42 and Initiate Neurite Outgrowth in Nerve Growth Factor-stimulated PC12 Cells[D]

Kazuhiro Aoki,* Takeshi Nakamura,* Keiko Fujikawa,† and Michiyuki Matsuda*

*Department of Tumor Virology, Research Institute for Microbial Diseases, Osaka University, Osaka 565-0871, Japan; and †Department of Biochemistry, Hokkaido University School of Medicine, Hokkaido 060-8638, Japan

Submitted October 18, 2004; Revised January 27, 2005; Accepted February 10, 2005
Monitoring Editor: Anne Ridley

Neurite outgrowth is an important process in the formation of neuronal networks. Rac1 and Cdc42, members of the Rho-family GTPases, positively regulate neurite extension through reorganization of the actin cytoskeleton. Here, we examine the dynamic linkage between Rac1/Cdc42 and phosphatidylinositol 3-kinase (PI3-kinase) during nerve growth factor (NGF)-induced neurite outgrowth in PC12 cells. Activity imaging using fluorescence resonance energy transfer probes showed that PI3-kinase as well as Rac1/Cdc42 was transiently activated in broad areas of the cell periphery immediately after NGF addition. Subsequently, local and repetitive activation of PI3-kinase and Rac1/Cdc42 was observed at the protruding sites. Depletion of Vav2 and Vav3 by RNA interference significantly inhibited both Rac1/Cdc42 activation and the formation of short processes leading to neurite outgrowth. At the NGF-induced protrusions, local phosphatidylinositol 3,4,5-trisphosphate accumulation recruited Vav2 and Vav3 to activate Rac1 and Cdc42, and conversely, Vav2 and Vav3 were required for the local activation of PI3-kinase. These observations demonstrated for the first time that Vav2 and Vav3 are essential constituents of the positive feedback loop that is comprised of PI3-kinase and Rac1/Cdc42 and cycles locally with morphological changes.

INTRODUCTION

Neurite outgrowth is of prime importance in the formation of neuronal networks. Rho-family GTPases (RhoA, Rac1, and Cdc42), which regulate actin dynamics in a diversity of cellular functions (Van Aelst and D'Souza-Schorey, 1997; Hall, 1998), also play central roles in neuronal morphogenesis during the development of neuronal networks (Mueller, 1999; Luo, 2000). Rac1 and Cdc42, implicated in the formation of lamellipodia and filopodia in nonneuronal cells, respectively (Hall, 1998), have been accepted as positive regulators of neurite outgrowth (Luo, 2000). Our recent study using fluorescence resonance energy transfer (FRET)-based probes has shown the localized and intermittent activation of Rac1 and Cdc42 within the neurite tips of PC12 cells stimulated with nerve growth factor (NGF) (Aoki *et al.*, 2004). This activation is largely dependent on phosphatidylinositol 3-kinase (PI3-kinase) activity, in agreement with the results of biochemical studies (Yasui *et al.*, 2001; Nusser *et al.*, 2002).

Activation of PI3-kinase has been shown to promote neurite outgrowth in NGF-stimulated PC12 cells and sympathetic neurons (Kobayashi *et al.*, 1997; Kuruvilla *et al.*, 2000) and also to support cell survival (Bibel and Barde, 2000; Kaplan and Miller, 2000). Although PI3-kinase is a multifunctional signaling molecule having various effectors (Cantley, 2002), a close linkage between Rac1/Cdc42 and PI3-kinase has been found in a wide range of morphological responses to external stimuli (Bourne and Weiner, 2002; Merlot and Firtel, 2003). Furthermore, a local positive feedback loop comprised of Rac1/Cdc42 and PI3-kinase has been hypothesized to be responsible for the symmetry breaking and persistent activation required for morphogenesis (Merlot and Firtel, 2003; Shi *et al.*, 2003). However, the spatiotemporal linkage between these two signaling modules is only poorly understood.

In the present study, we investigated this dynamic linkage between Rac1/Cdc42 and PI3-kinase during neurite outgrowth in PC12 cells stimulated with NGF. For this purpose, we used an RNA interference (RNAi) technique (Elbashir *et al.*, 2001; Brummelkamp *et al.*, 2002) and activity imaging using FRET probes (Mochizuki *et al.*, 2001; Itoh *et al.*, 2002). The former helps to identify guanine nucleotide exchange factors (GEFs) connecting PI3-kinase and Rac1/Cdc42 activation. The latter can monitor the spatiotemporal changes in activity of signaling molecules at neuritic processes cycling between extension and retraction. Our experiments showed

This article was published online ahead of print in *MBC in Press* (http://www.molbiolcell.org/cgi/doi/10.1091/mbc.E04–10–0904) on February 23, 2005.

[D] The online version of this article contains supplemental material at *MBC Online* (http://www.molbiolcell.org).

Address correspondence to: Takeshi Nakamura (t-nakamu@biken.osaka-u.ac.jp).

Abbreviations used: BSA, bovine serum albumin; CRIB, Cdc42/Rac1 interacting binding; CFP, cyan fluorescent protein; DIC, differential interference contrast; FRET, fluorescence resonance energy transfer; GEF, guanine nucleotide exchange factor; IMD, intensity-modulated display; NGF, nerve growth factor; PBS, phosphate-buffered saline; PI3-kinase, phosphatidylinositol 3-kinase; PIP_3, phosphatidylinositol 3,4,5-trisphosphate; RNAi, RNA interference; shRNA, short-hairpin RNA; YFP, yellow fluorescent protein.

that local phosphatidylinositol 3,4,5-trisphosphate (PIP_3) accumulation after NGF stimulation recruited Vav2 and Vav3 to the plasma membrane and thereby activated Rac1 and Cdc42; this Vav2/3-dependent activation of Rac1 and Cdc42 promoted the formation of short processes leading to neurite outgrowth. We also provide evidence that Vav2 and Vav3 are involved in the local activation of PI3-kinase at the protrusions after NGF stimulation. Therefore, this study demonstrates for the first time that Vav proteins are constituents of the PIP_3-dependent positive feedback loop that cycles locally with morphological changes.

MATERIALS AND METHODS

Plasmids

The plasmids encoding the FRET probes for small G proteins, Raichu-Rac1/1026 ×, Raichu-Cdc42/1061 × (Itoh *et al*., 2002; Yoshizaki *et al*., 2003), and Raichu-Ras/124 × (Ohba *et al*., 2003), have been described previously. cDNA of fllip-pm, FRET-base PIP_3 indicator, was generated according to Sato *et al*. (2003) and subcloned into the pCAGGS vector. The RNA targeting constructs were generated using pSUPER.retro.puro vector (OligoEngine, Seattle, WA). The 19-nucleotide sequences used to target rat Vav2, Vav3, Sos1, and Sos2 mRNAs were 5′-GTCGCTGCGGGAAGGTGAT-3′, 5′-GAGTCTGGAGAATATGCAA-3′, 5′-GCACTTCTCAACTTATCCC-3′, and 5′-GAGACTTGGAATTGCTTGA-3′, respectively. Mouse Vav2 cDNA (Kodama *et al*., 2000) was subcloned into the pCAGGS-FLAG vector. pCF1-Vav3-HA (Moores *et al*., 2000) was used for mouse Vav3 expression. N-terminally truncated active mutants of Vav2 and Vav3 (Δ186-Vav2 and Δ186-Vav3), lacking residues 1–186 (Bustelo, 2000), were subcloned into pERedNLS-FLAG, which contained the FLAG tag and an internal ribosomal entry site followed by the cDNA of Express Red (BD Biosciences, San Jose, CA) fused to nuclear localization signal at the 5′ side and 3′ side of the cloning site, respectively. Plekstrin homology (PH) domain-deletion mutants of Vav2 and Vav3 (Vav2ΔPH and Vav3ΔPH), lacking residues 387–506, were subcloned into pERedNLS-3HA, which contained the triple hemagglutinin (HA) tag in place of the FLAG tag of pERedNLS-FLAG. Cdc42/Rac1 interacting binding (CRIB) domain of PAK1 (amino acids 68–150) was inserted into the cloning site of the pIRM21-FLAG expression vector, which contained the FLAG tag and an internal ribosomal entry site followed by the cDNA of a red fluorescent protein, dsFP593, at the 5′ side and 3′ side of the cloning site, respectively (Aoki *et al*., 2004). pIRM21-FLAG-Ras-N17 has been described previously (Aoki *et al*., 2004).

Cells, Reagents, and Antibodies

PC12 cells were plated on 35-mm glass-base dishes (live imaging and immunocytochemistry; Asahi Techno Glass, Tokyo, Japan) or 60-mm plastic dishes (other studies) that were coated with collagen. The cells were maintained in RPMI 1640 medium (Invitrogen, Carlsbad, CA) supplemented with 10% horse serum and 5% fetal bovine serum. NGF and latrunculin B were purchased from Calbiochem (La Jolla, CA). Epidermal growth factor (EGF), LY294002, and puromycin were obtained from Sigma-Aldrich (St. Louis, MO). The following antibodies were used in this study: anti-Vav2 (H-200), anti-Sos2 (C-19), and anti-phospho-Vav2 (Tyr 172) polyclonal antibodies (Santa Cruz Biotechnology, Santa Cruz, CA); anti-phospho-Vav3 (Tyr 173) polyclonal antibody (BioSource International, Camarillo, CA); anti-tubulin monoclonal antibody (mAb) (Calbiochem); anti-Akt, anti-phospho-Akt (Thr308), anti-phospho-TrkA (Tyr 490), and anti-phospho-MAPK/ERK kinase (MEK)1/2 (Ser 217/221) polyclonal antibodies (Cell Signaling Technology, Beverly, MA); anti-Rac1, anti-Cdc42, anti-MEK1, anti-Sos1, and anti-phosphotyrosine (PY20) monoclonal antibodies (BD Transduction Laboratories, San Jose, CA); anti-FLAG M2 mAb (Sigma-Aldrich); anti-HA mAb (Roche Diagnostics, Indianapolis, IN); and Alexa 488 anti-mouse IgG, Alexa 488 anti-rat IgG, and Alexa 594 anti-rat IgG (Molecular Probes, Eugene, OR).

RNA Interference Experiments

PC12 cells were transfected with the desired pSUPER constructs by using LipofectAMINE 2000 (Invitrogen). After recovery, the cells were selected by 2-day incubation with 3 μg/ml puromycin and then used for further analysis. For FRET imaging, the indicated pRaichu plasmids were transfected into the short-hairpin RNA (shRNA)-expressing cells 1 d after the addition of puromycin as described above. After an additional 1-d incubation with puromycin, the cells were starved and used for imaging.

Reverse Transcription (RT)-PCR

Total RNA from PC12 cells expressing the indicated shRNAs was extracted by using Sepasol-RNA I super (Nacalai Tesque, Kyoto, Japan) and used for cDNA synthesis using a First-Strand cDNA synthesis kit (Amersham Biosciences, Piscataway, NJ). The forward rat Vav3 primer was 5′-TTAGGAACTACACTGGCACC-3′; the reverse primer was 5′-TTCTCCAGACTCTTTGGTCC-3′. Rat Vav3 cDNA was amplified for 30 cycles with the Expand High-Fidelity PLUS PCR system (Roche Diagnostics).

Time-Lapse Imaging

PC12 cells expressing FRET probes were starved for 6–12 h with phenol red-free DMEM/Ham's F-12 medium containing 0.1% bovine serum albumin (BSA) and then treated with 50 ng/ml NGF. The medium was covered with mineral oil (Sigma-Aldrich) to preclude evaporation. Cells were imaged with an IX71 inverted microscope (Olympus, Tokyo, Japan) equipped with a Cool SNAP-HQ cooled charge-coupled device camera (Roper Scientific, Trenton, NJ) controlled with MetaMorph software (Universal Imaging, West Chester, PA) as described previously (Mochizuki *et al*., 2001). The filters used for the dual-emission imaging studies were obtained from Omega Optical (Brattleboro, VT): an XF1071 (440AF21) excitation filter, an XF2034 (455DRLP) dichroic mirror, and two emission filters (XF3075 [480AF30] for cyan fluorescent protein [CFP] and XF3079 [535AF26] for yellow fluorescent protein [YFP]). Cells were illuminated with a 75-W Xenon lamp through a 12% neutral density filter and viewed through a 60 or 100× oil immersion objective lens. The exposure times for 4 × 4 binning were 400 ms for CFP and YFP images and 100 ms for differential interference contrast (DIC) images. After background subtraction, YFP/CFP ratio images were created with the MetaMorph software, and the images were used to represent FRET efficiency.

In Vitro Analysis of Rac1/Cdc42 Activation

The Rac1 and Cdc42 activities in mock- or NGF-treated cells were measured by the Bos' pull-down method according to Yasui *et al*. (2001). Briefly, cells were harvested in ice-cold lysis buffer (50 mM Tris, pH 7.5, 100 mM NaCl, 2 mM $MgCl_2$, 1% Nonidet P-40, 10% glycerol, 1 mM dithiothreitol, and 1 mM phenylmethylsulfonyl fluoride [PMSF]) containing GST-PAK-CRIB. The cleared lysates were incubated with glutathione-Sepharose beads (Amersham Biosciences) for 30 min at 4°C. The washed beads were boiled in sample buffer, and both the bound proteins and cell lysates were analyzed by immunoblotting with anti-Rac1 or anti-Cdc42 antibody. Blots were quantified with the luminescent image analyzer LAS 1000 Plus (Fuji Film, Tokyo, Japan). The amount of GTP-Rac1 or GTP-Cdc42 was divided by that of total Rac1 or Cdc42 in cell lysates, respectively. Then, the ratio of elevation of the amount of GTP-Rac1 or GTP-Cdc42 after NGF stimulation was used to examine the effect of depletion of Vav2/3 or Sos1/2.

Neurite Extension Assay

PC12 cells were transfected with the indicated pSUPER constructs and selected with 3 μg/ml puromycin for 2 d. Then, neurite outgrowth was stimulated with 50 ng/ml NGF and allowed to proceed for 60 h in DMEM/Ham's F-12 medium containing 0.1% BSA and 3 μg/ml puromycin. Quantification of neurite outgrowth was performed as described previously (Nakamura *et al*., 2002).

Immunocytochemistry

Cells were fixed with 3.7% formaldehyde and permeabilized with 0.2% Triton X-100. After having been soaked for 1 h in phosphate-buffered saline (PBS) containing 3% BSA and 0.02% Triton X-100, the samples were incubated for 1 h at room temperature with 5 μg/ml anti-FLAG M2 antibody or 1 μg/ml anti-HA antibody, washed with PBS, and then incubated for 30 min at room temperature with Alexa 488 anti-mouse IgG, Alexa 488 anti-rat IgG, or Alexa 594 anti-rat IgG, respectively. The samples were washed with PBS containing 0.2% Tween 20 and imaged with an FV-500 confocal microscope (Olympus, Tokyo, Japan)

Immunoprecipitation

Cells were harvested in ice-cold lysis buffer (25 mM Tris, pH 7.5, 150 mM NaCl, 1.5 mM $MgCl_2$, 1% Nonidet P-40, 10% glycerol, 1 mM EDTA, 1 mM EGTA, 2 mM sodium orthovanadate, 50 mM sodium fluoride, 1 mM PMSF, and 10 μg/ml aprotinin). The cleared lysates were incubated with 3 μg of anti-FLAG M2 antibody or 1 μg of anti-HA antibody. After 1.5-h tumbling at 4°C, protein G-Sepharose (Amersham Biosciences) was added, and incubation was continued for 1 h at 4°C. The washed beads were boiled in sample buffer, and the bound proteins were analyzed by immunoblotting.

RESULTS

Local Accumulation of PIP_3 at NGF-induced Protrusions

Our previous study demonstrating the PI3-kinase–dependent activation of Rac1 and Cdc42 at the protruding neurites of NGF-treated PC12 cells (Aoki *et al*., 2004) has prompted us to examine the spatiotemporal change of PI3-kinase activity at the NGF-induced protrusions (Figure 1). Fllip-pm (Sato *et al*., 2003), a FRET-based PIP_3 indicator, allows visualization

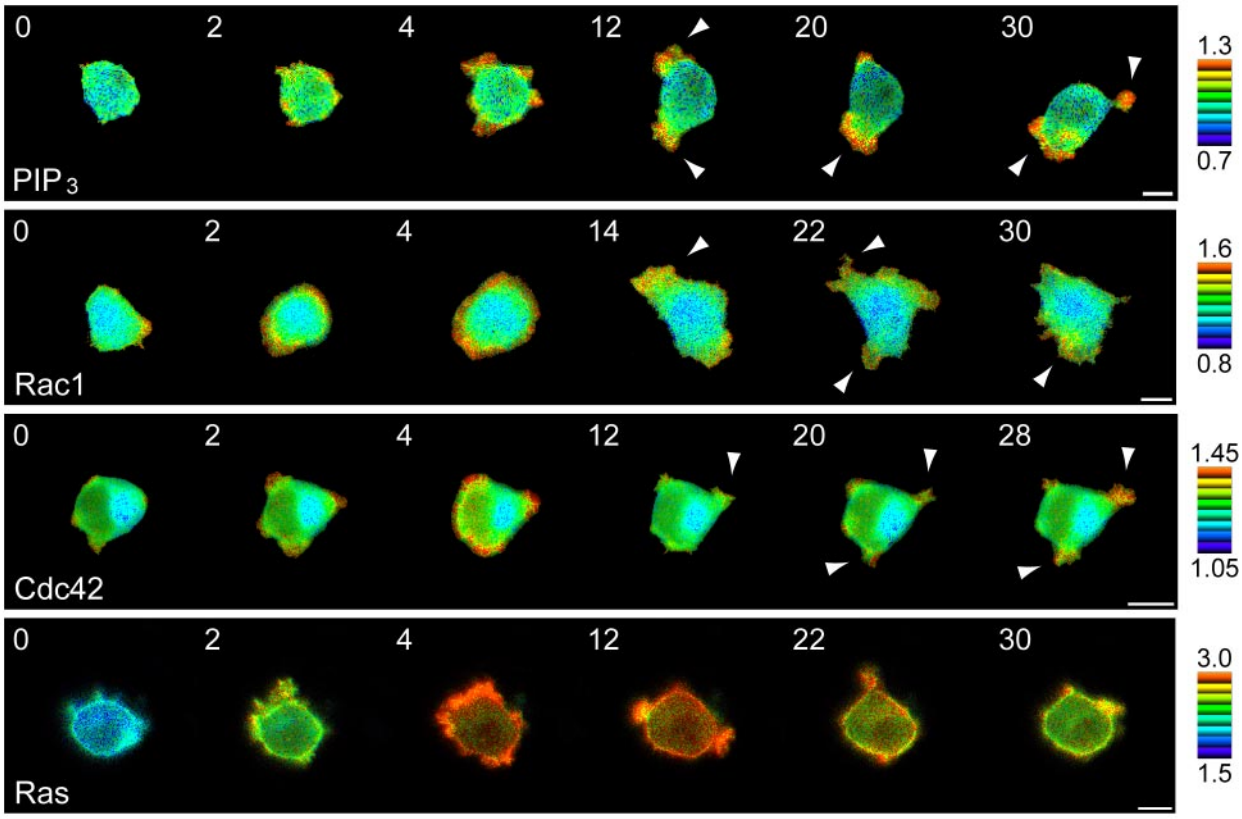

Figure 1. Spatiotemporal changes in PIP_3 concentration and Rac1/Cdc42/Ras activities upon NGF stimulation. PC12 cells expressing fllip-pm, Raichu-Rac1, Raichu-Cdc42, or Raichu-Ras were starved for 6 h and then treated with 50 ng/ml NGF. Images were obtained every 2 min for 30 min after NGF stimulation. Experiments were repeated at least five times for each probe. Representative ratio images of YFP/CFP at the indicated time points (minutes) after NGF addition are shown in the intensity-modulated display (IMD) mode. In the IMD mode, eight colors from red to blue are used to represent the YFP/CFP ratio, with the intensity of each color indicating the mean intensity of YFP and CFP. The upper and lower limits of the ratio image are shown on the right. Bars, 10 μm.

of PI3-kinase activity at the plasma membrane. PC12 cells expressing fllip-pm were imaged for YFP and CFP at an excitation wavelength of 440 nm. The YFP/CFP ratio reflects the FRET efficiency from CFP to YFP and correlates with the PIP_3 concentration (Sato *et al*., 2003). FRET imaging showed that the process of PI3-kinase activation was separated into early (0- to 10-min) and late (10- to 30-min) phases. In the early phase, PIP_3 levels increased transiently in broad areas at the cell periphery (Figure 1, top, 2–4 min). After this widespread PI3-kinase activation, local and repetitive PIP_3 accumulation was observed at the protruding sites in the late phase (arrowheads). For comparison, NGF-induced activation of Rac1, Cdc42, and Ras is also shown in Figure 1. The transient and widespread activation of PI3-kinase and Rac1/Cdc42 were similar in duration (<10 min), and local changes in Rac1/Cdc42 activity concurrent with a cycling of protrusion and retraction was very similar to the appearance of local PIP_3 accumulation in the late phase. In contrast, Ras activation was observed throughout the cells upon NGF stimulation and was sustained with a gradual decrease >30 min (bottom).

Depletion of Vav2 and Vav3 Attenuated NGF-dependent Activation of Rac1 and Cdc42

To identify a GEF(s) responsible for PI3-kinase–dependent activation of Rac1 and Cdc42, we used targeted depletion of candidate GEFs by RNA interference. Our recent work has suggested that NGF-induced activation of Rac1 and Cdc42 in PC12 cells is probably mediated by a common GEF(s) (Aoki *et al*., 2004). Candidates for such GEFs with dual specificity are Vav2 and Vav3, which activate a broad range of Rho GTPases, including Rac1 and Cdc42 (Han *et al*., 1998) in a variety of tissues (Schuebel *et al*., 1996; Movilla and Bustelo, 1999). We used an shRNA expression vector with the *pac* gene to allow selection of shRNA-expressing cells with puromycin. In Vav2 shRNA-expressing cells, >80% of endogenous Vav2 protein was depleted (Figure 2G, top). In Vav3 shRNA-expressing cells, RT-PCR analysis showed a >80% reduction in the level of endogenousVav3 mRNA (Figure 2G, middle). The silencing effect of Vav3 shRNA was confirmed by the efficient depletion of exogenous Vav3 protein (Figure 2G, bottom).

Depletion of Vav2 and Vav3 markedly inhibited NGF-induced activation of Rac1 and Cdc42 in PC12 cells. FRET imaging in control cells showed the widespread and transient activation of Rac1 and Cdc42 in the early phase (Figure 2A, middle, and B, gray zones). Subsequently, local and repetitive activation at the protrusions was observed in the late phase (Figure 2A, right, and B). However, in Vav2/3 double-knockdown cells, transient Rac1/Cdc42 activation in the early phase was significantly lower than that in control cells (Figure 2C, middle, and D, gray zones). We also noted that depletion of Vav2 and Vav3 suppressed the formation of lamellipodia (Figure 2, A and C, middle) and short pro-

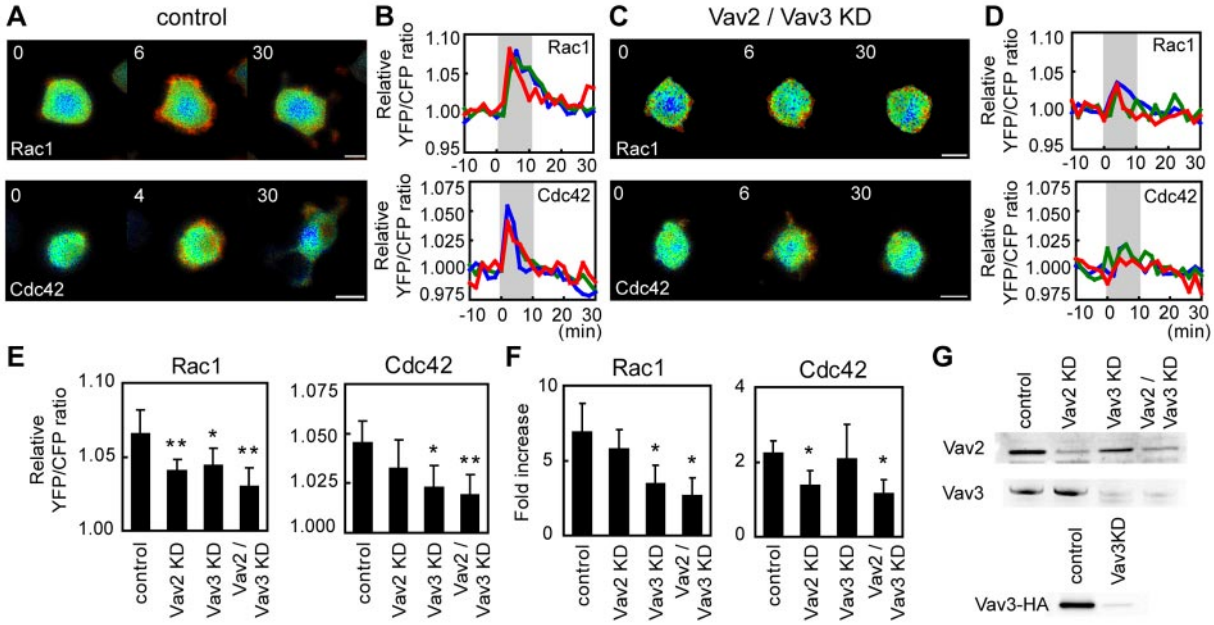

Figure 2. Effect of depletion of Vav2 and Vav3 on NGF-induced activation of Rac1 and Cdc42. (A–D) PC12 cells were transfected with an empty pSUPER vector (A and B) or both pSUPER-Vav2 and pSUPER-Vav3 (C and D). After selection with puromycin, the cells were further transfected with pRaichu-Rac1 (top) or pRaichu-Cdc42 (bottom). After serum starvation for 6 h, images were obtained every 2 min for 30 min after NGF stimulation. In A and C, representative ratio images of YFP/CFP at the indicated time points (minutes) after NGF addition are shown after normalization as follows. First, in each sample, we determined the average ratio over the whole cell before NGF addition and used that ratio as the reference value. Then, the raw YFP/CFP ratio of each pixel was divided by the reference value, and this normalized value was used to generate a normalized ratio image where the upper and lower limits of the ratio range were fixed at 1.15 and 0.85, respectively. Bars, 10 μm. In B and D, YFP/CFP ratios of three representative data sets were expressed by measuring the increase over the reference value used in A and C. Gray zones indicate the initial 10 min after NGF addition. (E) Bar graphs represent peak values of Rac1 (left) and Cdc42 (right) activation in control and knockdown cells. The average of the highest values of fold increase in the YFP/CFP ratio within 10 min of NGF addition is shown with SD. The number of cells examined for each sample was as follows: control (n = 6), Vav2 KD (n = 6), Vav3 KD (n = 5), Vav2/Vav3 KD (n = 7) for Rac1; control (n = 5), Vav2 KD (n = 5), Vav3 KD (n = 5), Vav2/Vav3 KD (n = 5) for Cdc42. The symbols indicate the results of *t* test analysis; *p $<$ 0.05, **p $<$ 0.01 compared with the control. (F) Control and knockdown cells were starved for 12 h, treated with or without NGF for 2.5 min, and examined by pull-down assay to detect active Rac1 (left) and Cdc42 (right). Experiments were repeated five times, and average values of fold increase compared with mock-treated cells are shown with standard deviations. The symbols indicate the results of *t* test analysis; *p $<$0.05 compared with the control. (G) Vav2 and Vav3 expression in control and knockdown cells were analyzed by immunoblotting (for Vav2, top) or RT-PCR analysis (for Vav3, middle). The efficiency of depletion of exogenous Vav3 protein by shRNA was confirmed by immunoblotting (bottom).

cesses (Figure 2, A and C, right). Detailed morphometric analysis is described below. Concurrent with the repression of process formation in Vav2/3-depleted cells, local Rac1/Cdc42 activation in the late phase also disappeared (Figure 2, A and C, right). Figure 2E shows the average increase in peak YFP/CFP ratios during the early phase in single- or double-knockdown cells. Reduced activation of Rac1 and Cdc42 was evident in Vav2 knockdown and Vav3 knockdown cells. Further suppression was observed in Vav2/3-depleted cells. These results were largely consistent with the results of the pull-down assay (Figure 2F). Together, both Vav2 and Vav3 are required for NGF-induced activation of Rac1 and Cdc42 in both early and late phases.

Effect of Depletion of Sos1 and Sos2 on NGF-dependent Rac1/Cdc42 Activation

Sos is implicated in NGF/TrkA signaling (Bibel *et al*., 2000; Kaplan *et al*., 2000) and has been shown to serve as a GEF for Rac in response to growth factor stimulation (Nimnual *et al*., 1998; Scita *et al*., 1999) in addition to its well known GEF activity toward Ras. Thus, we examined the role of Sos proteins (Sos1 and Sos2) in NGF-induced Rac1/Cdc42 activation by using shRNA expression vectors. Sos1 and Sos2 shRNAs efficiently reduced the amount of endogenous Sos1 and Sos2 proteins, respectively (Figure 3G). As expected, Ras activation upon NGF stimulation was inhibited almost completely in Sos1/2-depleted PC12 cells (Supplemental Figure 1A). In contrast, FRET imaging demonstrated that Rac1 activation upon NGF stimulation was unaffected by the depletion of either Sos1 or Sos2 (Figure 3, A–D, top, and E, left) in both early and late phases, whereas the pull-down assay showed a reduction of NGF-induced Rac1 activation in Sos1 knockdown cells (Figure 3F, left). The reason for this discrepancy is currently unknown (see *Discussion*). However, it is notable that Sos1/2-depleted cells showed essentially the same morphological change throughout early and late phases as did the control cells (Figure 3, A and C; described in detail in Figure 4). Therefore, we believe that Sos1 (and Sos2) is largely dispensable for Rac1 activation in NGF-stimulated PC12 cells. Unexpectedly, the transient Cdc42 activation in the early phase (Figure 3, A and B, bottom) was significantly suppressed in Sos1/2-depleted cells (Figure 3, C and D, bottom). Specifically, this suppression in knockdown cells was evident in cell bodies, whereas lamellipodial protrusions showed similar Cdc42 activation in the control and knockdown cells. This reduction in the

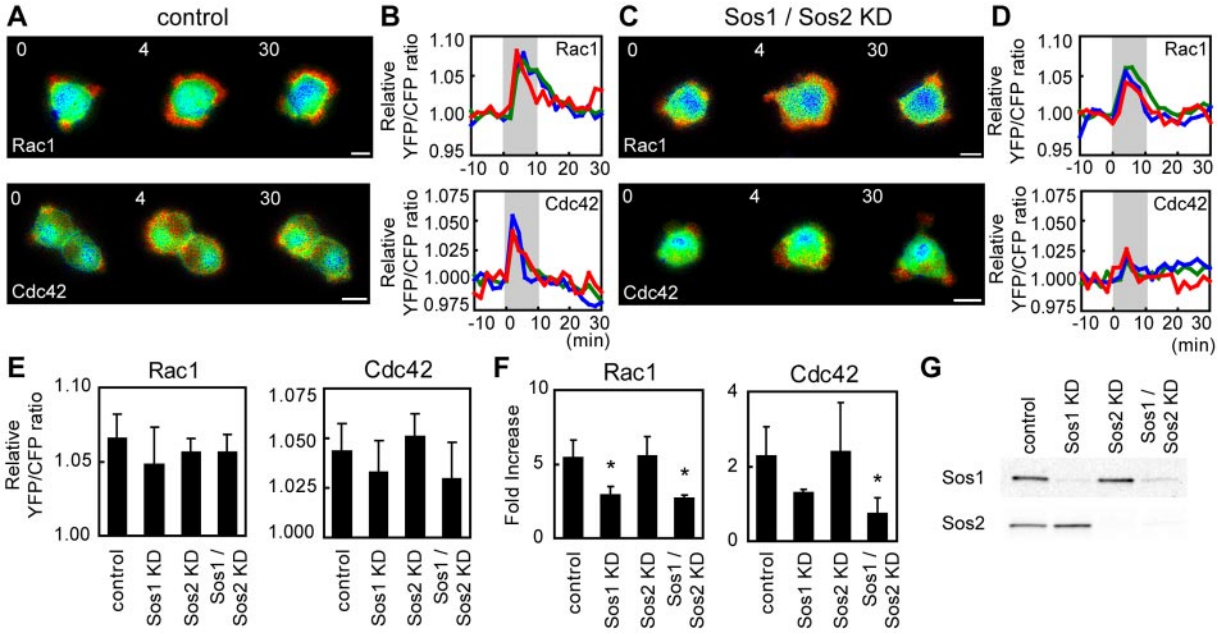

Figure 3. Effect of depletion of Sos1 and Sos2 on NGF-induced activation of Rac1 and Cdc42. (A–D) PC12 cells were transfected with an empty pSUPER vector (A and B) or both pSUPER-Sos1 and pSUPER-Sos2 (C and D). After puromycin selection, the cells were further transfected with pRaichu-Rac1 (top) or pRaichu-Cdc42 (bottom). After serum starvation, images were obtained every 2 min for 30 min after NGF stimulation. Representative time sequences of normalized ratio images of YFP/CFP (A and C) and line graphs of relative YFP/CFP ratios of three representative data sets (B and D) are shown, as described in the legend of Figure 2, A–D. Bars, 10 μm. (E) Bar graphs represent peak values of Rac1 (left) and Cdc42 (right) activation in control and knockdown cells as in Figure 2E. The number of cells examined for each sample was as follows: control (n = 6), Sos1 KD (n = 5), Sos2 KD (n = 5), Sos1/Sos2 KD (n = 5) for Rac1; control (n = 5), Sos1 KD (n = 7), Sos2 KD (n = 6), Sos1/Sos2 KD (n = 5) for Cdc42. The symbols indicate the results of *t* test analysis; *p $<$ 0.05 compared with the control. (F) Control and knockdown cells were starved for 12 h, treated with or without NGF for 2.5 min, and examined by pull-down assay to detect active Rac1 (left) and Cdc42 (right). Experiments were repeated three times, and average values of fold increase compared with mock-treated cells are shown with standard deviations. The symbols indicate the results of *t* test analysis; *p $<$ 0.05 compared with the control. (G) Sos1 and Sos2 expression in control and knockdown cells were analyzed by immunoblotting.

early phase came from the lack of Sos1 expression (Figure 3, E and F), although the signaling pathway from Sos1 to Cdc42 remains to be elucidated (see *Discussion*). In the late phase, depletion of Sos proteins did not inhibit the formation of short processes and local Cdc42 activation (Figure 3, C and D, bottom). Therefore, NGF-induced Cdc42 activation by Sos1 was restricted to the cell bodies in the early phase.

Vav2 and Vav3 Are Required for Induction of Neuritic Processes and PI3-Kinase Activation

To obtain further evidence of the engagement of Vav2 and Vav3 in NGF-induced neurite outgrowth, we performed time-lapse recording of morphological changes of the first 3 h after NGF addition. Control cells showed rapid cycling of protrusion and retraction in response to NGF (Figure 4A, top). Depletion of Vav2 and Vav3 severely inhibited the formation of short processes (Figure 4A, middle, and B); this observation was in agreement with the reduced activation of Rac1 and Cdc42 in Vav2/3 double-knockdown cells throughout early and late phases (Figure 2). In contrast, the lack of Sos1/2 expression did not affect the morphological change that occurred during the initial 3 h after NGF addition (Figure 4A, bottom, and B). Figure 4C shows that NGF enhanced PC12 cell migration; however, this enhancement was completely abolished in Vav2/3-depleted cells. This agrees with previous results showing enhanced migration of Vav2 or Vav3-overexpressing fibroblasts (Liu and Burridge, 2000; Sachdev *et al*., 2002).

Local PIP_3 accumulation at the NGF-induced protrusions (Figure 1) and the marked decrease in these protrusions by depletion of Vav2 and Vav3 (Figure 4) prompted us to examine the PI3-kinase activity upon NGF stimulation in Vav2/3 knockdown cells. In the early phase ($<$10 min), PI3-kinase activation was almost comparable between the control and Vav2/3 knockdown cells (Figure 5, A and B). However, in the late phase, the appearance of PIP_3 accumulation was significantly reduced in Vav2/3-depleted cells in comparison with the control (Figure 5, A and B). In addition, the NGF-induced increase in Akt phosphorylation, generally used as an indicator of PI3-kinase activity, was reduced in the late phase in Vav2/3 knockdown cells compared with the control (Figure 5C). Therefore, Vav2 and Vav3 are implicated in the local activation of PI3-kinase at the protrusions after NGF stimulation. In contrast, there was no significant difference in PIP_3 accumulation and Akt phosphorylation between the control and Sos1/2-depleted cells (Figure 5, A–C). These data demonstrated the presence of a positive feedback loop that comprises PI3-kinase, Vav2/3, and Rac1/Cdc42 at the NGF-induced protrusions (Figure 8). The signaling linkage of Vav proteins to PI3-kinase has been reported in hematopoietic cells (Inabe *et al*., 2002; Reynolds *et al*., 2002; Vigorito *et al*., 2004); however, the mechanism by which Vav proteins activate PI3-kinase remains unknown. Thus, to obtain mechanistic insight into the Vav-PI3-kinase link in PC12 cells, we used the CRIB domain of PAK and the dominant negative mutant of Ras (Supplemental Figure 2A).

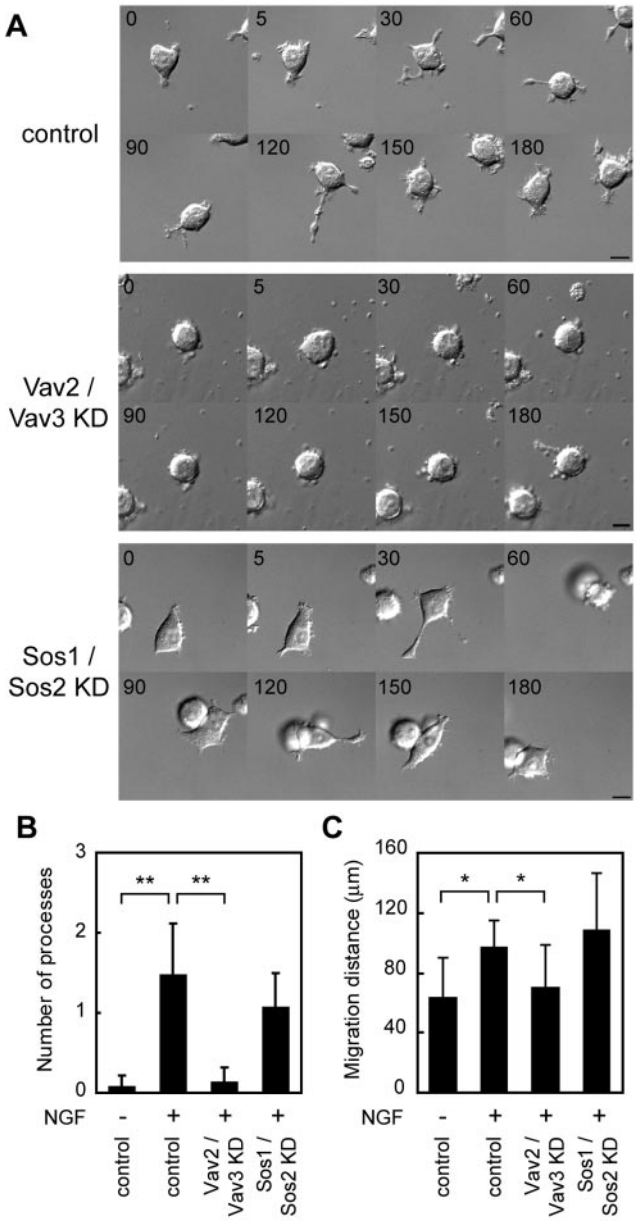

Figure 4. Effect of Vav2/3 or Sos1/2 depletion on the initial morphological change after NGF stimulation. PC12 cells were transfected with an empty pSUPER vector, pSUPER-Vav2 and pSUPER-Vav3, or pSUPER-Sos1 and pSUPER-Sos2. After recovery, the cells were incubated with puromycin for 2 d. After serum starvation, the cells were stimulated with NGF, and DIC images were obtained every 5 min for 3 h. Experiments were repeated at least five times for each sample. (A) Representative images of the control cells (top), Vav2/3-depleted cells (middle), and Sos1/2-depleted cells (bottom) are shown at the indicated time points (minutes) after NGF addition. Bars, 10 μm. (B and C) Quantification of NGF-induced protrusions and migration in control, Vav2/3- or Sos1/2-depleted cells. Bars represent (B) the average of the number of protrusions longer than 10 μm at three time points (1, 2, and 3 h after NGF addition) and (C) the average length of the trajectories of nuclei during 3 h. Control cells without NGF treatment also were examined. The symbols indicate the results of *t* test analysis; *$p < 0.05$, **$p < 0.01$ compared with the control.

The expression of N-terminally-truncated active mutants of Vav2 and Vav3 (Δ186-Vav2 and Δ186-Vav3) increased the PIP_3 concentration in PC12 cells. This increase was reduced by one-half in the cells coexpressing PAK-CRIB, whereas the Ras-N17 coexpression had no effect on the PI3-kinase activation by Δ186-Vav2 and Δ186-Vav3. These data indicated that Rac1 and Cdc42, not Ras, mainly mediate the signals from Vav2/3 to PI3-kinase. Furthermore, Supplemental Figure 2B showed that disruption of actin filament with latrunculin B significantly perturbed the NGF-induced activation of PI3-kinase only in the late phase, suggesting that actin cytoskeleton is implicated in a cycling of positive feedback loop comprised of PI3-kinase, Vav2/3, and Rac1/Cdc42.

Depletion of Vav2/3 and Sos1/2 Inhibited NGF-induced Neurite Outgrowth

Next, we examined NGF-induced formation of mature neurites in knockdown cells. The PC12 cells transfected with an empty pSUPER vector developed neurites within 60 h of treatment with NGF (Figure 6A, left). In contrast, depletion of Vav2/3 as well as that of Sos1/2 strongly inhibited neurite outgrowth (Figure 6A, middle and right). The proportions of neurite-bearing cells were calculated in control and knockdown cells (Figure 6B). In control cells, the proportion of neurite-bearing cells was 55% in the presence of NGF. However, only 12% of Vav2/3 knockdown cells bore neurites even in the presence of NGF; this is consistent with the decrease in NGF-induced Rac1/Cdc42 activation and protrusions by depletion of Vav2 and Vav3 (Figures 2 and 4). Depletion of Sos1 and Sos2 also significantly reduced NGF-induced neurite outgrowth. This is probably because the Ras/Raf/MEK/extracellular signal-regulated kinase (Erk) pathway, which has been shown to be required for neurite extension mainly through transcriptional regulation (Markus *et al*., 2002), was severely inhibited in Sos1/2-depleted cells. In fact, the level of NGF-induced MEK activation was reduced by >60% in Sos1/2 knockdown cells compared with control cells (Supplemental Figure 1B).

NGF Induced PI3-Kinase-dependent Translocation of Vav2 and Vav3 to the Plasma Membrane

To clarify the mechanism of Vav2/3 activation upon NGF stimulation, we first examined the subcellular distribution of Vav proteins in response to NGF. The PC12 cells expressing FLAG-tagged Vav2 or HA-tagged Vav3 were mock treated or treated with NGF for 2.5 min and then stained with anti-FLAG or anti-HA antibody, respectively (Figure 7A). In the absence of NGF, Vav2 and Vav3 were mainly cytoplasmic. On NGF stimulation, a large part of Vav2 and Vav3 were translocated to the plasma membrane (Figure 7, A and B). It is noteworthy that the NGF-induced translocation of Vav2 and Vav3 was abolished by pretreatment with LY294002. Furthermore, Vav2 and Vav3 mutants lacking their PH domains could not relocate to the plasma membrane in response to NGF (Supplemental Figure 3). These results were consistent with the previous observation that NGF-induced Rac1/Cdc42 activation was largely dependent on PI3-kinase activity (Yasui *et al*., 2001; Nusser *et al*., 2002; Aoki *et al*., 2004). In PC12 cells, EGF also recruited Vav2 and Vav3 to the plasma membrane; however, the EGF-dependent translocation was inhibited neither by LY294002 treatment (Figure 7, A and B) nor the absence of the PH domain (Supplemental Figure 3).

Another key event modulating the activity of the Vav family is tyrosine phosphorylation (Bustelo, 2000; Hornstein *et al*., 2004). PC12 cells expressing Vav2 or Vav3 cDNA were mock treated or treated with NGF or EGF and lysed for immunoprecipitation. On EGF stimulation, the increase in tyrosine-phosphorylation of Vav2/3 and their association with EGFR were clearly detected (Figure 7C), as shown

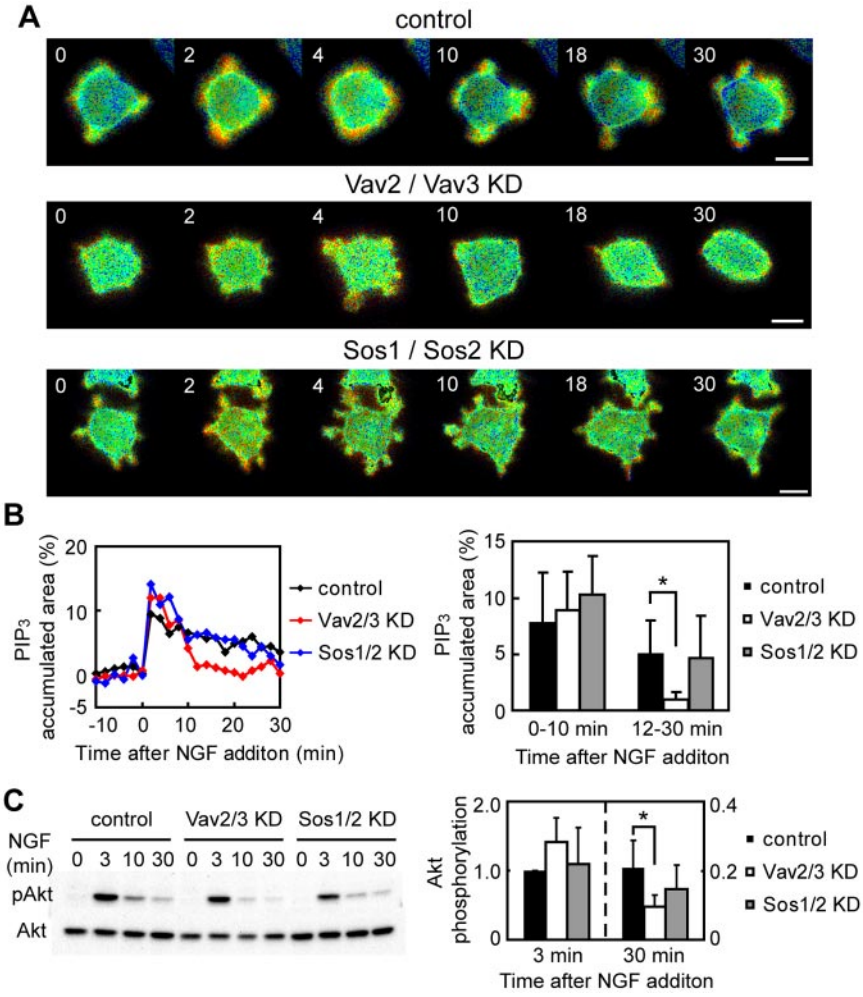

Figure 5. Inhibition of PIP_3 accumulation by depletion of Vav2 and Vav3. PC12 cells were transfected with an empty pSUPER vector, both pSUPER-Vav2 and pSUPER-Vav3 or both pSUPER-Sos1 and pSUPER-Sos2. After selection with puromycin, the cells were transfected with the plasmid encoding flip-pm. After serum starvation for 6 h, images were obtained every 2 min for 30 min after NGF stimulation. (A) Representative time-sequences of normalized ratio images of YFP/CFP are shown as described in the legend to Figure 2,A and C. Bars, 10 μm. (B) PIP_3-accumulated area was calculated using MetaMorph software as follows: In each sample, we determined the average ratio over the whole cell before NGF stimulation and used that ratio as the reference value. Then, the percentage of the area where the local YFP/CFP ratio exceeded the reference value by at least 10% was measured at each time point after NGF stimulation. Left, time-dependent changes of the average PIP_3-accumulated area of control (n = 5), Vav2/Vav3 KD (n = 5), and Sos1/Sos2 KD (n = 6) cells. Bar graph (right) illustrates the average of PIP_3-acculated area with SD for the initial 10-min period and the succeeding 20-min period. The symbols indicate the results of *t* test analysis; *$p < 0.05$, **$p < 0.01$ compared with the control. (C) PC12 cells transfected with pSUPER, both pSUPER-Vav2 and pSUPER-Vav3, or both pSUPER-Sos1 and pSUPER-Sos2 were serum starved and stimulated with NGF for the indicated periods. Cell lysates were immunoblotted with anti-phospho Akt (Thr308) antibody and anti-Akt antibody (left). Akt phosphorylation was expressed as an average of the ratio of each sample to the control cells stimulated for 3 min (right). The symbols indicate the results of *t* test analysis (*$p < 0.05$, **$p < 0.01$; n = 4).

earlier in Cos7 and NIH3T3 cells (Moores *et al*., 2000). On the other hand, Figure 7C and Supplemental Figure 4 showed a comparable level of weak tyrosine-phosphorylation of Vav2 and Vav3 in the absence or presence of NGF. Together, NGF-induced Vav2/3 activation was concurrent with the PI3-kinase–dependent membrane recruitment and did not accompany the elevation of their tyrosine phosphorylation.

DISCUSSION

Here, we have shown that Vav2 and Vav3 play a critical role in Rac1/Cdc42 activation and promote neurite outgrowth in NGF-stimulated PC12 cells. Previous studies have shown that several RhoGEFs are implicated in various aspects of neuronal morphogenesis (Luo, 2000). For example, Trio and Ephexin have been shown to play essential roles in activating RhoGTPases during growth cone guidance (O'Brien *et al*., 2000; Shamah *et al*., 2001). Tiam1 is required for neurite outgrowth in N1E-115 neuroblastoma cells and hippocampal neurons (Leeuwen *et al*., 1997; Kunda *et al*., 2001). Among these RhoGEFs, Vav2 and Vav3 are unique in that they are constituents of a PIP_3-dependent positive feedback loop concurrent with morphological change (Figure 8). In the early phase response (0–10 min), widespread increase in PIP_3 resulted in recruitment of Vav2 and Vav3, thereby activating Rac1 and Cdc42 in broad areas. The PIP_3 positive-feedback loop was not yet established. In the late phase (10–30 min), localized and repetitive PIP_3 accumulation and PI3-kinase–dependent Rac1/Cdc42 activation was observed at the protrusions. The appearance of local PIP_3 accumulation depended on Vav2/3 expression. Thus, a positive feedback loop comprised of PI3-kinase, Vav2/3, and Rac1/Cdc42 cycled at the protrusions in the late phase. Therefore, the mechanism of NGF-induced Rac1/Cdc42 activation was different between the early and late phases (Figure 8); this difference has been uncovered by taking advantage of FRET imaging, which can monitor spatiotemporal changes in activities.

A PIP_3-dependent positive feedback loop plays a central role in symmetry breaking leading to morphological change (Bourne and Weiner, 2002). This feedback loop has been mostly studied in leukocytes (Wang *et al*., 2002; Weiner *et al*., 2002) and *Dictyostelium* (Iijima *et al*., 2002), and it is proposed to be a functional module in a wide range of chemotactic response and morphogenesis during development (Merlot and Firtel, 2003; Shi *et al*., 2003). Interestingly, neutrophils acquire morphological polarity even under a uniform concentration of chemoattractant (Srinivasan *et al*., 2003). This self-organizing polarity resembles the NGF-induced neurite outgrowth examined here in that global PI3-kinase activation was initially observed and subsequently changed to asymmetric activation. However, some differences should

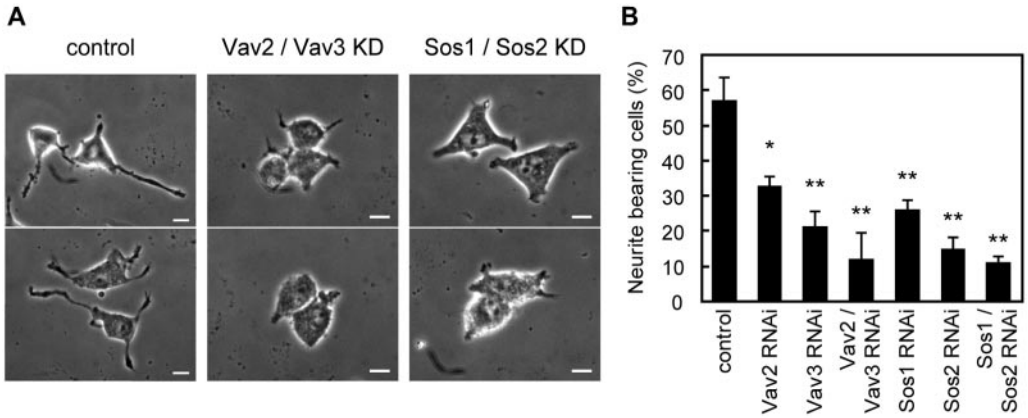

Figure 6. Effect of depletion of Vav2, Vav3, Sos1, or Sos2 on NGF-induced neurite outgrowth. PC12 cells were transfected with the indicated pSUPER constructs and incubated with puromycin for 2 d. Then, the selected cells were cultured with NGF for 60 h and fixed for microscopy. (A) Representative phase contrast images of control cells (left), Vav2/3-depleted cells (middle), and Sos1/2-depleted cells (right). Bars, 10 μm. (B) Cells having neurites whose lengths were twofold longer than their cell body lengths were scored as neurite-bearing cells. At least 60 cells were assessed in each experiment, and the experiments were repeated three times. The results are expressed as the mean percentage of neurite-bearing cells with the SD. The symbols indicate the results of *t* test analysis; *$p < 0.05$, **$p < 0.01$ compared with the control.

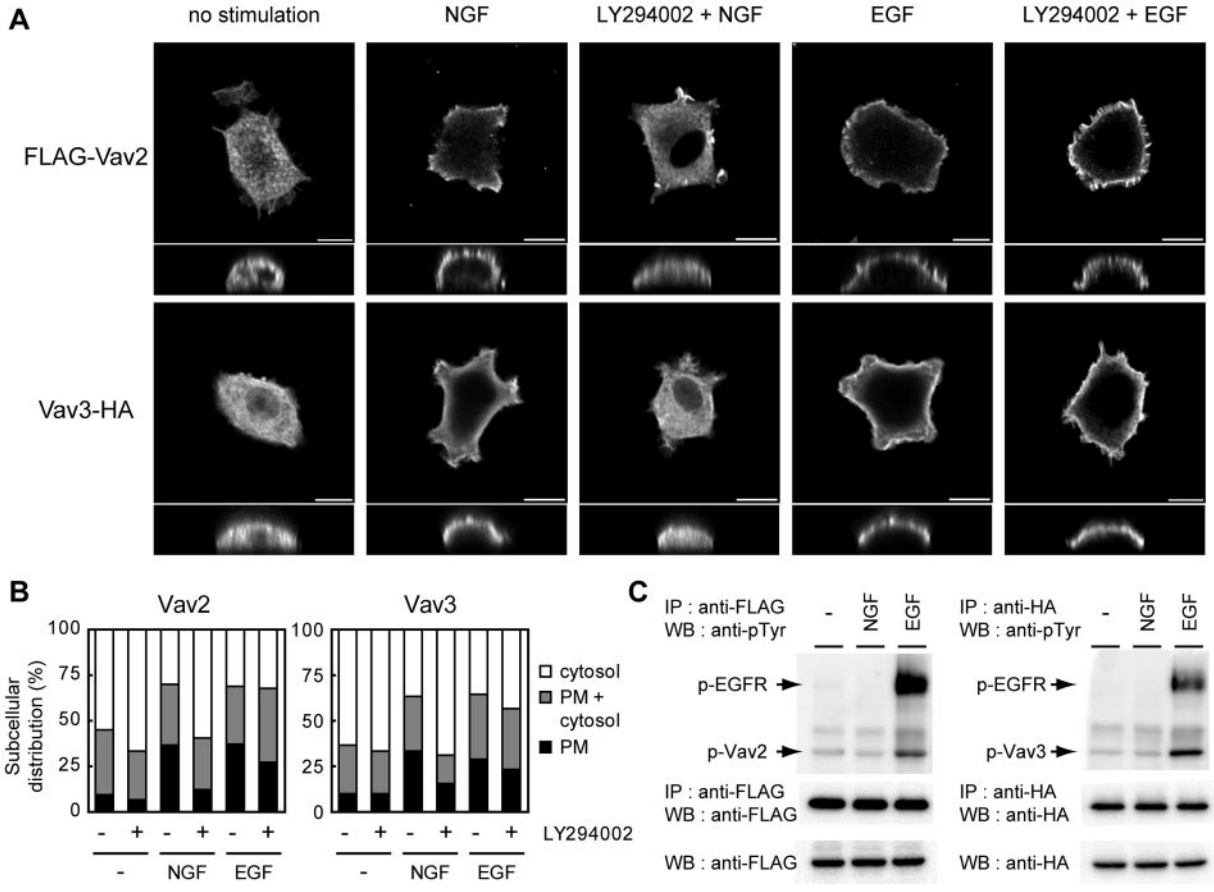

Figure 7. Membrane recruitment of Vav2 and Vav3 in PC12 cells stimulated with NGF or EGF. (A and B) Serum-starved PC12 cells expressing FLAG-Vav2 or Vav3-HA were pretreated with or without 20 μM LY294002 (Yasui *et al*., 2001) for 30 min. Then, the cells were mock treated or treated with 50 ng/ml NGF or 50 ng/ml EGF for 2.5 min, and stained with anti-FLAG (for Vav2) or anti-HA (for Vav3) antibody. (A) Representative confocal images of horizontal and vertical sections are shown with scale bars (10 μm). (B) The subcellular distribution of Vav2 and Vav3 was classified into three categories: mainly at the plasma membrane (PM), both at the plasma membrane and cytosol (PM + cytosol), or mainly in the cytosol. Composite bar graphs show the percentage of number of the cells in each category for samples indicated below the graph. At least 30 cells were examined in each sample. (C) PC12 cells were transfected with FLAG-Vav2 or Vav3-HA cDNA. After serum starvation, cells were mock treated or treated with NGF or EGF for 2.5 min. Anti-FLAG immunoprecipitates (left) were immunoblotted with anti-phosphotyrosine or anti-FLAG (for Vav2 detection) antibody. Anti-HA immunoprecipitates (right) were probed with anti-phosphotyrosine or anti-HA (for Vav3 detection) antibody.

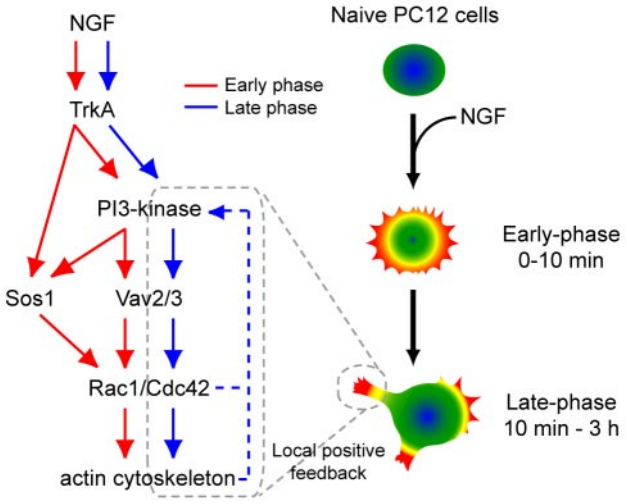

Figure 8. Schematic representation of signaling pathway of NGF-induced neurite outgrowth in PC12 cells. In the early phase (0–10 min), global activation of PI3-kinase upon NGF stimulation recruited Vav2 and Vav3 to activate Rac1/Cdc42 in broad areas. Lamellipodial protrusion at the cell periphery was concomitantly observed. Sos1 partially mediated Cdc42 activation only in cell bodies immediately after NGF addition. In the late phase (10–30 min), NGF/TrkA signaling drives a cycling of positive feedback loop comprised of PI3-kinase, Vav2/3, Rac1/Cdc42, and actin cytoskeleton; this feedback loop promotes neurite outgrowth by regulating morphological dynamics.

be noted. First, in neutrophils, the PIP_3-dependent feedback loop is established immediately after stimulation, because the expression of a dominant negative mutant of Rac1 abolished the initial global activation of PI3-kinase (Srinivasan *et al.*, 2003). In contrast, Rac1/Cdc42 activation was not required for PI3-kinase activation during the early phase in PC12 cells (Figure 5). Second, migrating leukocytes form a leading edge, predominantly consisting of lamellipodia; consistently, the PIP_3-dependent feedback loop in neutrophils was dependent on the activity of Rac1 but not of Cdc42 (Srinivasan *et al.*, 2003). By contrast, neurite tips in PC12 cells as well as growth cones of primary neurons consist of both lamellipodia and filopodia. Furthermore, the actin organization in growth cone periphery markedly differs from the regular Y branch structures in lamellipodial extension of nonneuronal cells (Svitkina and Borisy, 1999; Meyer and Feldman, 2002). These large differences in cell morphology might impose distinct signaling mechanisms on leukocytes and neuronal cells.

Vav proteins are activated through relief of intramolecular inhibitory domains; this relief is performed in multiple ways such as tyrosine phosphorylation and PIP_3 binding to the PH domain (Bustelo, 2000; Hornstein *et al.*, 2004). Figure 7 and Supplemental Figure 3 showed that NGF-induced Vav2/3 activation was concurrent with their PI3-kinase–dependent translocation to the plasma membrane through the PH domains. Although many earlier studies have claimed the critical importance of tyrosine phosphorylation of Vav family members in their activation (Crespo *et al.*, 1997; Han *et al.*, 1997; Hornstein *et al.*, 2004), the increase in tyrosine phosphorylation of Vav2/3 upon NGF stimulation was not detected in PC12 cells (Figure 7 and Supplemental Figure 4). Similarly, Vav2-mediated Rac1 activation was required for cell spreading in NIH3T3 cells; nevertheless, a concomitant increase in tyrosine phosphorylation of Vav2 was not observed (Marignani and Carpenter, 2001). Furthermore, treatment of COS7 cells with the PI3-kinase inhibitor before EGF stimulation decreased Vav2 activation without the change of its tyrosine phosphorylation (Tamás *et al.*, 2003). In fact, in the presence of PIP_3, the nonphosphorylated DH-PH domain of Vav1 bound to Rac1 (Das *et al.*, 2000). PIP_3 binding to the PH domains and the concomitant change of conformation are known to up-regulate other RhoGEFs such as Sos1 and P-Rex1 (Schmidt and Hall, 2002); our data support the similar possibility for activation mechanism of Vav2 and Vav3 upon NGF stimulation. In addition, scaffolding function of Vav proteins (Bustelo, 2001) may contribute to Rac1/Cdc42 activation and morphological changes. The mechanism of Vav2/3 activation in neuronal cells is far less understood in comparison with that in hematopoietic cells. And it has been argued that activation mechanism of Vav proteins varies depending on the type of cells or ligands (Bustelo, 2000). Therefore, further mechanistic investigation in neuronal cells is required.

Depletion of Sos1 and Sos2 markedly inhibited NGF-induced neurite outgrowth (Figure 6). Although Sos proteins can exert a GEF activity toward both Ras and Rac (Nimnual and Bar-Sagi, 2002), we think that the inhibited neurite extension is primarily due to the inhibition of the Ras pathway by the following reasoning. First, signaling through the Ras/Raf/MEK/Erk pathway leads to appropriate changes in gene expression for promoting neurite outgrowth (Markus *et al.*, 2002). NGF up-regulates the expression levels of cytoskeletal components and regulators (peripherin, coffilin, and MAP4) and signaling molecules accelerating neurite extension (Trio, RhoG, and p35) (Troy *et al.*, 1992; Angelastro *et al.*, 2000; Katoh *et al.*, 2000; Harada *et al.*, 2001; Estrach *et al.*, 2002). It is likely that the Ras/Erk pathway mediates much of this up-regulation, and their shutdown eliminates neurite outgrowth. Second, the lack in Sos1/2 expression did not affect the morphological change in the initial 3 h after NGF addition (Figure 5). Therefore, it is implausible that Sos proteins contribute to the PIP_3-dependent positive feedback loop at the NGF-induced protrusions, although a reduction of NGF-induced Cdc42 activation in Sos1-depleted cells was observed (Figure 3). This reduced Cdc42 activation cannot be explained by aborted activation of Ras/PI3-kinase signaling in Sos1 knockdown cells because the bulk of PI3-kinase activity is mediated by Gab1 independently of Ras pathway in NGF-stimulated PC12 cells (Holgado-Madruga *et al.*, 1997). To our knowledge, the signaling pathway from Sos1 to Cdc42 is yet to be described and will be the subject of future study. Actually, we repeatedly observed that the knockdown of Vav2 and Vav3 could not completely inhibit the NGF-induced activation of Rac1 and Cdc42 (Figure 2, A–F). It may be partly explained by the Sos1-induced Cdc42 activation, and furthermore, we could not exclude the possibility that other GEFs additionally contribute to Rac1/Cdc42 activation upon NGF stimulation.

All results obtained here by pull-down assay were consistent with that by FRET imaging except for the discrepancy found in NGF-induced Rac1 activation in Sos1-depleted cells (Figure 3). Although the precise reason for this discrepancy is not clear, we should note that both methods have drawbacks. The FRET probe for Rac1 monitors the balance between GEF and GTPase-activating protein activities, but it is insensitive to Rho guanine nucleotide dissociation inhibitor (RhoGDI) activity (Itoh *et al.*, 2002). However, we previously showed that RhoGDI did not contribute significantly to the regulation of Rac1/Cdc42 activity in NGF-stimulated PC12 cells by using another type of FRET probe (Aoki *et al.*, 2004). On the other hand, solubilization is potentially prob-

lematic in pull-down assays. Because cells are highly heterogeneous, it is possible that some fractions are readily solubilized in standard lysis buffer, whereas others are not. If long-term depletion of Sos1 affects the partition of active Rac1 upon stimulation, this change can be accidentally detected by pull-down assay. To settle this discrepancy, an independent study is required. Thus, we performed morphometric analysis (Figure 4) and found that depletion of Sos1/2 did not affect the NGF-induced morphological changes; this result was consistent with that of FRET imaging.

This study for the first time demonstrated that Vav2 and Vav3 are constituents of the PIP_3-dependent positive feedback loop concurrent with morphological change. It is tempting to propose that the involvement of Vav proteins in similar feedback loops can be found in a wide range of morphological responses. In hematopoietic cells, the signaling linkage of Vav proteins to PI3-kinase has been reported previously (Inabe *et al*., 2002; Reynolds *et al*., 2002; Vigorito *et al*., 2004); however, the implication of the Vav-PI3-kinase link for a positive feedback loop is yet to be addressed, and the mechanism by which Vav proteins activate PI3-kinase remains unknown. We demonstrated that, in NGF-treated PC12 cells, Rac1 and Cdc42, not Ras, mainly mediate the signals from Vav2/3 to PI3-kinase (Supplemental Figure 1A). Intact actin cytoskeleton also is required for the positive feedback loop comprised of PI3-kinase, Vav2/3, and Rac1/Cdc42 (Supplemental Figure 1B). The organized actin filament by active Rac1/Cdc42 may either directly contribute to PI3-kinase activation or keep the machinery of the positive feedback loop in a concentrated state. In a future study, these two possibilities could be distinguished by deducing a quantitative linkage among central elements of the PIP_3-dependent feedback loop, including cytoskeletal components by monitoring densely the spatiotemporal change of their activities and concentrations. Furthermore, based on such a quantitative analysis, we could expect to elucidate both a general framework for the PIP_3-dependent positive feedback loop and the specific mechanisms devised to perform a variety of morphological responses from yeast and mold to vertebrate immune and nervous systems.

ACKNOWLEDGMENTS

We thank Dr. Y. Takai for providing the Vav2 cDNA and Dr. E. Hara for advice on the RNAi experiment. We are also grateful to N. Yoshida, N. Fujimoto, K. Fukuhara, and Y. Matsuura for technical assistance and to members of the Matsuda laboratory for technical advice and helpful input. This work was supported by grants-in-aid from the Ministry of Education, Science, Sports and Culture of Japan and a grant from the Health Science Foundation, Japan.

REFERENCES

Angelastro, J. M., Klimaschewski, L., Tang, S., Vitolo, O. V., Weissman, T. A., Donlin, L. T., Shelanski, M. L., and Greene, L. A. (2000). Identification of diverse nerve growth factor-regulated genes by serial analysis of gene expression (SAGE) profiling. Proc. Natl. Acad. Sci. USA *97*, 10424–10429.

Aoki, K., Nakamura, T., and Matsuda, M. (2004). Spatio-temporal regulation of Rac1 and Cdc42 activity during nerve growth factor-induced neurite outgrowth in PC12 cells. J. Biol. Chem. *279*, 713–719.

Bibel, M., and Barde, Y. A. (2000). Neurotrophins: key regulators of cell fate and cell shape in the vertebrate nervous system. Genes Dev. *14*, 2919–2937.

Bourne, H. R., and Weiner, O. (2002). A chemical compass. Nature *419*, 21.

Brummelkamp, T. R., Bernards, R., and Agami, R. (2002). A system for stable expression of short interfering RNAs in mammalian cells. Science *296*, 550–553.

Bustelo, X. R. (2000). Regulatory and signaling properties of the Vav family. Mol. Cell. Biol. *20*, 1461–1477.

Bustelo, X. R. (2001). Vav proteins, adaptors and cell signaling. Oncogene *20*, 6372–6381.

Cantley, L. C. (2002). The Phosphoinositide 3-Kinase Pathway. Science *296*, 1655–1657.

Crespo, P., Schuebel, K. E., Ostrom, A. A., Gutkind, J. S., and Bustelo, X. R. (1997). Phosphotyrosine-dependent activation of Rac-1 GDP/GTP exchange by the Vav proto-oncogene product. Nature *385*, 169–172.

Das, B., Shu, X., Day, G. J., Han, J., Krishna, U. M., Falck, J. R., and Broek, D. (2000). Control of intramolecular interactions between the pleckstrin homology and Dbl homology domains of Vav and Sos1 regulates Rac binding. J. Biol. Chem. *275*, 15074–15081.

Elbashir, S. M., Harborth, J., Lendeckel, W., Yalcin, A., Weber, K., and Tuschl, T. (2001). Duplexes of 21-nucleotide RNAs mediate RNA interference in cultured mammalian cells. Nature *411*, 494–498.

Estrach, S., Schmidt, S., Diriong, S., Penna, A., Blangy, A., Fort, P., and Debant, A. (2002). The human Rho-GEF trio and its target GTPase RhoG are involved in the NGF pathway, leading to neurite outgrowth. Curr. Biol. *12*, 307–312.

Hall, A. (1998). Rho GTPases and the actin cytoskeleton. Science *279*, 509–514.

Han, J., Das, B., Wei, W., Van Aelst, L., Mosteller, R. D., Khosravi-Far, R., Westwick, J. K., Der, C. J., and Broek, D. (1997). Lck regulates Vav activation of members of the Rho family of GTPases. Mol. Cell. Biol. *17*, 1346–1353.

Han, J., Luby-Phelps, K., Das, B., Shu, X., Xia, Y., Mosteller, R. D., Krishna, U. M., Falck, J. R., White, M. A., and Broek, D. (1998). Role of substrates and products of PI 3-kinase in regulating activation of Rac-related guanosine triphosphatases by Vav. Science *279*, 558–560.

Harada, T., Morooka, T., Ogawa, S., and Nishida, E. (2001). ERK induces p35, a neuron-specific activator of Cdk5, through induction of Egr1. Nat. Cell Biol. *3*, 453–459.

Holgado-Madruga, M., Moscatello, D. K., Emlet, D. R., Dieterich, R., and Wong, A. J. (1997). Grb2-associated binder-1 mediates phosphatidylinositol 3-kinase activation and the promotion of cell survival by nerve growth factor. Proc. Natl. Acad. Sci. USA *94*, 12419–12424.

Hornstein, I., Alcover, A., and Katzav, S. (2004). Vav proteins, masters of the world of cytoskeleton organization. Cell Signal. *16*, 1–11.

Iijima, M., Huang, Y. E., and Devreotes, P. (2002). Temporal and spatial regulation of chemotaxis. Dev. Cell *3*, 469–478.

Inabe, K., Ishiai, M., Scharenberg, A. M., Freshney, N., Downward, J., and Kurosaki, T. (2002). Vav3 modulates B cell receptor responses by regulating phosphoinositide 3-kinase activation. J. Exp. Med. *195*, 189–200.

Itoh, R. E., Kurokawa, K., Ohba, Y., Yoshizaki, H., Mochizuki, N., and Matsuda, M. (2002). Activation of Rac and Cdc42 video imaged by fluorescent resonance energy transfer-based single-molecule probes in the membrane of living cells. Mol. Cell. Biol. *22*, 6582–6591.

Kaplan, D. R., and Miller, F. D. (2000). Neurotrophin signal transduction in the nervous system. Curr. Opin. Neurobiol. *10*, 381–391.

Katoh, H., Yasui, H., Yamaguchi, Y., Aoki, J., Fujita, H., Mori, K., and Negishi, M. (2000). Small GTPase RhoG is a key regulator for neurite outgrowth in PC12 cells. Mol. Cell. Biol. *20*, 7378–7387.

Kobayashi, M., *et al*. (1997). Expression of a constitutively active phosphatidylinositol 3-kinase induces process formation in rat PC12 cells. J. Biol. Chem. *272*, 16089–16092.

Kodama, A., Matozaki, T., Fukuhara, A., Kikyo, M., Ichihashi, M., and Takai, Y. (2000). Involvement of an SHP-2-Rho small G protein pathway in hepatocyte growth factor/scatter factor-induced cell scattering. Mol. Biol. Cell *11*, 2565–2575.

Kunda, P., Paglini, G., Quiroga, S., Kosik, K., and Caceres, A. (2001). Evidence for the involvement of Tiam1 in axon formation. J. Neurosci. *21*, 2361–2372.

Kuruvilla, R., Ye, H., and Ginty, D. D. (2000). Spatially and functionally distinct roles of the PI3-K effector pathway during NGF signaling in sympathetic neurons. Neuron *27*, 499–512.

Leeuwen, F. N., Kain, H.E.T., Kammen, R. A., Michiels, F., Kranenburg, O. W., and Collard, J. G. (1997). The guanine nucleotide exchange factor Tiam1 affects neuronal morphology; opposing roles for the small GTPases Rac and Rho. J. Cell Biol. *139*, 797–807.

Liu, B. P., and Burridge, K. (2000). Vav2 activates Rac1, Cdc42, and RhoA downstream from growth factor receptors but not β1 integrins. Mol. Cell. Biol. *20*, 7160–7169.

Luo, L. (2000). Rho GTPases in neuronal morphogenesis. Nat. Rev. Neurosci. *1*, 173–180.

Marignani, P. A., and Carpenter, C. L. (2001). Vav2 is required for cell spreading. J. Cell Biol. *154*, 177–186.

Markus, A., Patel, T. D., and Snider, W. D. (2002). Neurotrophic factors and axonal growth. Curr. Opin. Neurobiol. *12*, 523–531.

Merlot, S., and Firtel, R. A. (2003). Leading the way: directional sensing through phosphatidylinositol 3-kinase and other signaling pathways. J. Cell Sci. *116*, 3471–3478.

Meyer, G., and Feldman, E. L. (2002). Signaling mechanisms that regulate actin-based motility processes in the nervous system. J. Neurochem. *83*, 490–503.

Mochizuki, N., Yamashita, S., Kurokawa, K., Ohba, Y., Nagai, T., Miyawaki, A., and Matsuda, M. (2001). Spatio-temporal images of growth-factor-induced activation of Ras and Rap1. Nature *411*, 1065–1068.

Moores, S. L., Selfors, L. M., Fredericks, J., Breit, T., Fujikawa, K., Alt, F. W., Brugge, J. S., and Swat, W. (2000). Vav family proteins couple to diverse cell surface receptors. Mol. Cell. Biol. *20*, 6364–6373.

Movilla, N., and Bustelo, X. R. (1999). Biological and regulatory properties of Vav-3, a new member of the Vav family of oncoproteins. Mol. Cell. Biol. *19*, 7870–7885.

Mueller, B. K. (1999). Growth cone guidance: first steps towards a deeper understanding. Annu. Rev. Neurosci. *22*, 351–388.

Nakamura, T., Komiya, M., Sone, K., Hirose, E., Gotoh, N., Morii, H., Ohta, Y., and Mori, N. (2002). Grit, a GTPase-activating protein for the Rho family, regulates neurite extension through association with the TrkA. receptor and N-Shc and CrkL/Crk adapter molecules. Mol. Cell. Biol. *22*, 8721–8734.

Nimnual, A., and Bar-Sagi, D. (2002). The two hats of SOS. Sci. STKE *2002*, pe36.

Nimnual, A. S., Yatsula, B. A., and Bar-Sagi, D. (1998). Coupling of Ras and Rac guanosine triphosphatases through the Ras exchanger Sos. Science *279*, 560–563.

Nusser, N., Gosmanova, E., Zheng, Y., and Tigyi, G. (2002). Nerve growth factor signals through TrkA, phosphatidylinositol 3-kinase, and Rac1 to inactivate RhoA during the initiation of neuronal differentiation of PC12 cells. J. Biol. Chem. *277*, 35840–35846.

O'Brien, S. P., Seipel, K., Medley, Q. G., Bronson, R., Segal, R., and Streuli, M. (2000). Skeletal muscle deformity and neuronal disorder in Trio exchange factor-deficient mouse embryos. Proc. Natl. Acad. Sci. USA *97*, 12074–12078.

Ohba, Y., Kurokawa, K., and Matsuda, M. (2003). Mechanism of the spatio-temporal regulation of Ras and Rap1. EMBO J. *22*, 859–869.

Reynolds, L. F., Smyth, L. A., Norton, T., Freshney, N., Downward, J., Kinoussis, D., and Tybulewicz, V.L.J. (2002). Vav1 transduced T cell receptor signals to the activation of phospholipase C-γ1 via phosphoinositide 3-kinase-dependent and -independent pathways. J. Exp. Med. *195*, 1103–1114.

Sachdev, P., Zeng, L., and Wang, L. H. (2002). Distinct role of phosphatidylinositol 3-kinase and Rho family GTPases in Vav3-induced cell transformation, cell motility, and morphological changes. J. Biol. Chem. *277*, 17638–17648.

Sato, M., Ueda, Y., Takagi, T., and Umezawa, Y. (2003). Production of PtdInsP3 at endomembranes is triggered by receptor endocytosis. Nat. Cell Biol. *5*, 1016–1022.

Schmidt, A., and Hall, A. (2002). Guanine nucleotide exchange factors for Rho GTPases: turning on the switch. Genes Dev. *16*, 1587–1609.

Schuebel, K. E., Bustelo, X. R., Nielsen, D. A., Song, B. J., Barbacid, M., Goldman, D., and Lee, I. J. (1996). Isolation and characterization of murine Vav2, a member of the Vav family of proto-oncogenes. Oncogene *13*, 363–371.

Scita, G., Nordstrom, J., Carbone, R., Tenca, P., Giardina, G., Gutkind, S., Bjarnegard, M., Betsholtz, C., and Di Fiore, P. P. (1999). EPS8 and E3B1 transduce signals from Ras to Rac. Nature *401*, 290–293.

Shamah, S. M., *et al*. (2001). EphA receptors regulate growth cone dynamics through the novel guanine nucleotide exchange factor Ephexin. Cell *105*, 233–244.

Shi, S. H., Jan, L. Y., and Jan, Y. N. (2003). Hippocampal neuronal polarity specified by spatial localized mPar3/mPar6 and PI 3-kinase activity. Cell *112*, 63–75.

Srinivasan, S., Wang, F., Glavas, S., Ott, A., Hofmann, F., Aktories, K., Kalman, D., and Bourne, H. R. (2003). Rac and Cdc42 play distinct roles in regulating PI(3,4,5)P3 and polarity during neutrophil chemotaxis. J. Cell Biol. *160*, 375–385.

Svitkina, T. M., and Borisy, G. G. (1999). Arp2/3 complex and actin depolymerizing factor/cofilin in dendritic organization and treadmilling of actin filament array in lamellipodia. J. Cell Biol. *145*, 1009–1026.

Tamás, P., Solti, Z., Bauer, P., Illés, A., Sipeki, S., Bauer, A., Faragó, A., Downward, J., and Buday, L. (2003). Mechanism of EGF regulation of Vav2, a guanine nucleotide exchange factor for Rac. J. Biol. Chem. *278*, 5163–5171.

Troy, C. M., Greene, L. A., and Shelanski, M. L. (1992). Neurite outgrowth in peripherin-depleted PC12 cells. J. Cell Biol. *117*, 1085–1092.

Van Aelst, L., and D'Souza-Schorey, C. (1997). Rho GTPases and signaling networks. Genes Dev. *11*, 2295–2322.

Vigorito, E., Bardi, G., Glassford, J., Lam, E. W., Clayton, E., and Turner, M. (2004). Vav-dependent and Vav-independent phosphatidylinositol 3-kinase activation in murine B cells determined by the nature of the stimulus. J. Immunol. *176*, 3209–3214.

Wang, F., Herzmark, P., Weiner, O. D., Srinivasan, S., Servant, G., and Bourne, H. R. (2002). Lipid products of PI(3)Ks maintain persistent cell polarity and directed motility in neutrophils. Nat. Cell Biol. *4*, 513–518.

Weiner, O. D., Neilsen, P. O., Prestwich, G. D., Kirschner, M. W., Cantley, L. C., and Bourne, H. R. (2002). A PtdInsP(3)- and Rho GTPase-mediated positive feedback loop regulates neutrophil polarity. Nat. Cell Biol. *4*, 509–513.

Yasui, H., Katoh, H., Yamaguchi, Y., Aoki, J., Fujita, H., Mori, K., and Negishi, M. (2001). Differential responses to nerve growth factor and EGF in neurite outgrowth of PC12 cells are determined by Rac1 activation systems. J. Biol. Chem. *276*, 15298–15305.

Yoshizaki, H., Ohba, Y., Kurokawa, K., Itoh, R. E., Nakamura, T., Mochizuki, N., Nagashima, K., and Matsuda, M. (2003). Activity of Rho-family G proteins during cell division as visualized with FRET-based probes. J. Cell Biol. *162*, 223–232.